JACS
JOURNAL OF THE AMERICAN CHEMICAL SOCIETY
Article
pubs.acs.org/JACS

Time-Resolved IR Spectroscopy Reveals a Mechanism with TiO_2 as a Reversible Electron Acceptor in a TiO_2–Re Catalyst System for CO_2 Photoreduction

Mohamed Abdellah,*[,†,‡] Ahmed M. El-Zohry,[†] Liisa J. Antila,[†] Christopher D. Windle,[§] Erwin Reisner,[§] and Leif Hammarström*[,†]

[†]Ångström Laboratory, Department of Chemistry, Uppsala University, Box 523, 75120 Uppsala, Sweden
[‡]Department of Chemistry, Qena Faculty of Science, South Valley University, 83523 Qena, Egypt
[§]Christian Doppler Laboratory for Sustainable SynGas Chemistry, Department of Chemistry, University of Cambridge, Lensfield Road, Cambridge CB2 1EW, United Kingdom

Supporting Information

ABSTRACT: Attaching the phosphonated molecular catalyst $[Re^{I}Br(bpy)(CO)_3]^0$ to the wide-bandgap semiconductor TiO_2 strongly enhances the rate of visible-light-driven reduction of CO_2 to CO in dimethylformamide with triethanolamine (TEOA) as sacrificial electron donor. Herein, we show by transient mid-IR spectroscopy that the mechanism of catalyst photoreduction is initiated by ultrafast electron injection into TiO_2, followed by rapid (ps-ns) and sequential two-electron oxidation of TEOA that is coordinated to the Re center. The injected electrons can be stored in the conduction band of TiO_2 on an ms-s time scale, and we propose that they lead to further reduction of the Re catalyst and completion of the catalytic cycle. Thus, the excited Re catalyst gives away one electron and would eventually get three electrons back. The function of an electron reservoir would represent a role for TiO_2 in photocatalytic CO_2 reduction that has previously not been considered. We propose that the increase in photocatalytic activity upon heterogenization of the catalyst to TiO_2 is due to the slow charge recombination and the high oxidative power of the Re^{II} species after electron injection as compared to the excited MLCT state of the unbound Re catalyst or when immobilized on ZrO_2, which results in a more efficient reaction with TEOA.

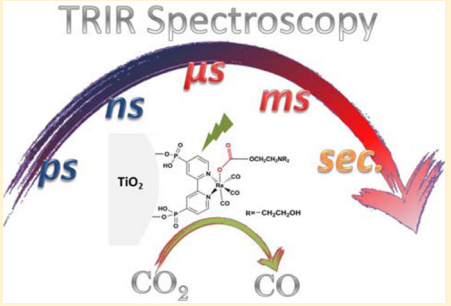

INTRODUCTION

Tremendous efforts have been put toward exploring new energy resources to face the problems of energy shortage and global warming. A continuous increase of the CO_2 concentration in the atmosphere is the main reason behind global warming.[1] A smart solution is to convert CO_2 emissions to fuels or other useful chemicals, which is one of the goals of artificial photosynthesis.[2−10] Photocatalytic and photoelectrocatalytic reduction of CO_2 has been achieved by employing metals and semiconductors[11−13] or enzymes bound to photoelectrodes.[14,15] The former suffers from poor selectivity, and conversely, the latter shows excellent selectivity but suffers from stability issues.[14,15] Balancing between both high selectivity and stability can potentially be achieved using a synthetic molecular catalyst for CO_2 reduction.[7,10,11,16−20] Generally, there are two approaches to CO_2 photoreduction with synthetic molecular catalysts. In the first, the catalyst receives electrons from a photosensitizer after excitation. In the second, the catalyst itself plays a dual role, working as both photosensitizer and catalyst as exemplified by the rhenium tricarbonyl bipyridine bromide $[Re^{I}Br(bpy)(CO)_3]^0$ catalyst (Figure S1A).[7,20]

Recently, some of us attached this catalyst to an n-type TiO_2 semiconductor via phosphonic acid linker groups (TiO_2–[Re(2,2′-bipyridine-4,4′-bisphosphonic acid)$(CO)_3$(L)], where initially L = Br^- but is replaced during the photoreaction; Scheme 1). In the presence of triethanolamine (TEOA) as electron donor, this leads to a higher yield (TON) of CO_2 photoreduction compared to both the homogeneous system without TiO_2 and to systems where the same catalyst was attached to other metal oxides, such as ZrO_2.[21] TiO_2 was proposed to stabilize reduced catalyst intermediates and hinder formation of unreactive Re−Re dimers but not participate directly in the electron transfer reactions.

In the present study, we attempt to answer several questions to understand the role of TiO_2 and to propose the photoreduction mechanism of the attached catalyst. First, is TiO_2 unreactive or is the excited $[ReBr(bpy)(CO)_3]$ oxidized by electron injection into TiO_2, as has been shown in some cases?[22] Second, what are the roles of the TEOA in the photocatalytic process? Finally, what is the role of TiO_2 in the photoreduction process? To answer these questions, we used

Received: October 31, 2016
Published: December 24, 2016

DOI: 10.1021/jacs.6b11308
J. Am. Chem. Soc. 2017, 139, 1226−1232

Scheme 1. Ligand Exchange Process Combined with CO_2 Capture of the $[Re^I(bpy)(CO)_3DMF]^+$ Ccatalyst in TEOA/CO_2 Solution

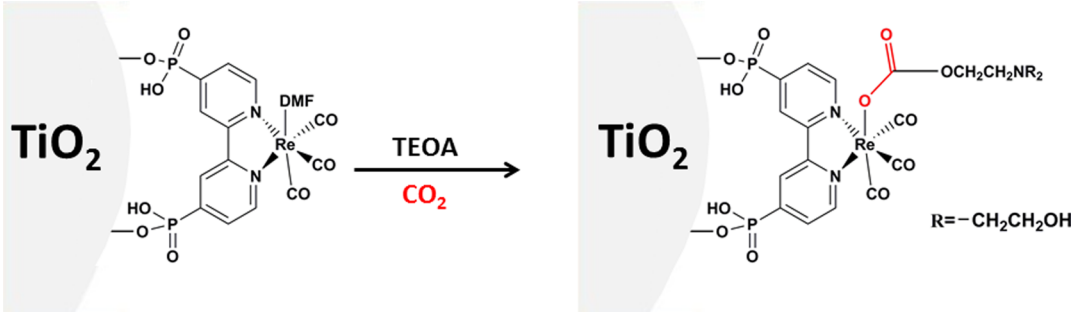

time-resolved IR (TRIR) in the region of CO stretching vibrations from time scales of femtoseconds up to seconds. ν(CO) is very sensitive to the electron density of the central Re ion, allowing us to identify and follow the Re excited state and different oxidation states.[23−25]

EXPERIMENTAL SECTION

Steady-State Spectroscopy. Steady-state absorption and emission were recorded using a Varian Cary 5000 and a Horiba Jobin Yvon Fluorolog, respectively. The emission spectrum for $[Re^IBr(bpy)(CO)_3]^0$ in DMF was corrected for the wavelength-dependent instrument sensitivity and measured at the right angle using a 1 cm quartz cuvette. IR spectrum for $[Re^IBr(bpy)(CO)_3]^0$ in DMF was recorded in a modified Omni cell (Specac) with O-ring sealed CaF_2 windows and a path length of 100 μm using a Bruker IFS 66v/S FTIR spectrophotometer controlled by OPUS softwear. IR spectra for TiO_2−$[Re^I(bpy)(CO)_3DMF]^+$ on CaF_2 films were measured directly using the same setup. For the ligand exchange to be monitored in the presence of TEOA and CO_2, the attached catalyst on TiO_2 films (on CaF_2) was immersed into a DMF/TEOA (5:1) mixture with continuous CO_2 bubbling.

Ultrafast Transient Mid-IR Absorption Spectroscopy. The 1 mJ, 45 fs output of a 1 kHz Ti:sapphire amplifier (Spitfire Pro, Spectra-Physics) was split into two separate commercial optical parametric amplifiers (TOPAS-C, Light Conversion), which generate the visible pump at 418 nm and the mid-IR probe (1850−2200 cm^{-1}) pulses. Prior to reaching the sample, the probe beam was split into equal intensity probe and reference beams using a wedged ZnSe window. Both beams pass through the sample, but only the probe beam interacts with the photoexcited volume of the sample. All beams are focused with a single f = 10 cm off axis parabolic mirror to an ∼70 μm spot size in the sample. The pump intensity was attenuated to 650 μW. The probe and reference beams were dispersed by a commercial monochromator (Triax 190, HORIBA Jobin Yvon) equipped with a 75 groove/mm grating and detected on a dual array, 2 × 64 pixel mercury cadmium telluride detector (InfraRed Associated, Inc.). The instrument response function for the experiments was approximately 100 fs. The sample was mounted in a Harrick flow cell.[26]

Transient Mid-IR Absorption Spectroscopy. A frequency doubled Q-switched Nd:YAG laser (Quanta-Ray ProSeries, Spectra-Physics) was employed to obtain 355 nm pump light, 10 mJ/pulse with a fwhm of 10 ns. The 355 nm pump light was used through the MOPO crystal to generate 440 nm light to pump the sample. Probing was done with the continuous wave quantum cascade (QC) IR laser with a tuning capability between 1960 and 2150 cm^{-1} (Daylight Solutions). For IR detection, a liquid nitrogen-cooled mercurycadmium-telluride (MCT) detector (KMPV10-1-J2, Kolmar Technologies, Inc.) was used. The IR probe light was overlapped with the pump beam in a quasi-*co*-linear arrangement at 25° angle. Transient absorption traces were acquired with a Tektronix TDS 3052 500 MHz (5GS/s) oscilloscope in connection with the L900 software (Edinburgh Instruments) and processed using Origin 9 software.[27,28]

For the spectroscopy measurements, 2 mg of the catalyst was dissolved in 10 mL of DMF; then, mesoporous TiO_2 (anatase nanoparticles with average size ∼20 nm and bandgap ∼3.2 eV) films were immersed in this solution for the sensitization process for 20 h while the photocatalytic measurements were carried out for the colloidal TiO_2−catalyst hybrid system.[21] The catalyst has a broad MLCT band at λ = 380 nm followed by an ultraviolet band below 350 nm due to ligand-centered transitions.[29] The MLCT band stays the same after the attachment to TiO_2 (Figure S1B).[24] The MLCT state generates a characteristic broad emission band at λ = 600 nm for the triplet state $^3(Re)^*$ (see inset of Figure S1B). The FTIR spectrum for TiO_2−$[Re^I(bpy)(CO)_3DMF]$ shows the stretching vibration of the $(CO)_3$ groups at 2041 and 1934 cm^{-1}, which confirms (i) the attachment of the catalyst on the TiO_2 surface and (ii) the replacement of the Br ligand with the DMF ligand on the surface of TiO_2 (Figure S1C). The stretching vibration of the $(CO)_3$ groups shifts from 2024 and 1882 cm^{-1} for the Br version to higher wavenumbers due to the formation of the DMF version.[21,30]

RESULTS AND DISCUSSION

Electron Injection from Excited $[Re^I(bpy)(CO)_3DMF]^*$ to TiO_2. To investigate the electron injection from the excited catalyst $[Re^I(bpy)(CO)_3DMF]^*$ to TiO_2, we first used the same sensitization conditions to attach the catalyst to ZrO_2 (noninjecting semiconductor as a reference).[31] Then, we used fs-TRIR to test the electron injection process. The ZrO_2−$[Re^I(bpy)(CO)_3DMF]^+$ system shows the typical spectral features of the excited $[Re^I(bpy)(CO)_3]^*$: the bleach of the ground state CO bands (GSB) at ∼2040 cm^{-1} and around 1960 cm^{-1} and the corresponding excited-state bands (ESA) at ∼2057 cm^{-1} and around 2010 cm^{-1} (Figure 1A).[32] In addition to these spectral features, the TiO_2−$[Re^I(bpy)(CO)_3DMF]^+$ system shows (i) a new peak on the higher wavenumber side compared to the ground state bleach (GSB) due to the oxidized state of the catalyst $[Re^{II}(bpy)(CO)_3DMF]^{2+}$ (at 2088 cm^{-1})[25] and (ii) a broad absorption band in the entire probe region due to electrons in the TiO_2 conduction band (CB)($TiO_2(e^-)$−$[Re^{II}(bpy)(CO)_3DMF]^{2+}$)[22,25] (Figure 1B). The amplitude of both the oxidized catalyst $[Re^{II}(bpy)(CO)_3]^{2+}$ peak and the electrons in the TiO_2 CB increase with increasing delay time with no decay up to 5 ns. Thus, there is no observable charge recombination on this time scale, but instead, there is a slow additional component of electron injection. The traces at 2088 cm^{-1} (oxidized catalyst after background subtraction of e^-_{CB} signal) and at 2125 cm^{-1} (e^-_{CB} signal) have different kinetics (Figure S2B). The electron trace shows significant appearance of the e^-_{CB} signal on an ∼2 ps time scale, whereas the oxidized catalyst peak growth is slower (∼30 ps). This difference could be because the electron signal is very strong and initially buries the oxidized catalyst peak. The catalyst peak is initially broad

DOI: 10.1021/jacs.6b11308
J. Am. Chem. Soc. 2017, 139, 1226−1232

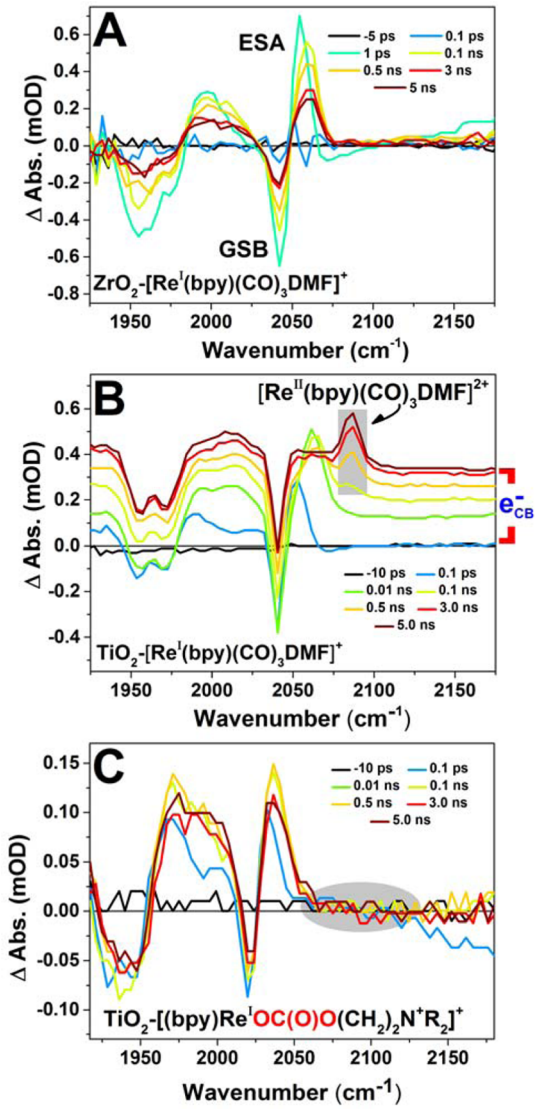

Figure 1. (A) fs-TRIR for the ZrO_2–$[Re^I(bpy)(CO)_3]^+$ system in DMF, (B) fs-TRIR for the TiO_2–$[Re^I(bpy)(CO)_3]^+$ system without TEOA, and (C) fs-TRIR for the TiO_2–$[Re^I(bpy)(CO)_3$-$OC(O)O$-$(CH_2)_2N^+R_2]^+$ system in DMF/TEOA solution (5:1) and CO_2 bubbling (the absorption at 2100 cm^{-1} was subtracted from the spectra to emphasize molecular signals).

but narrows with time and is thus more clearly seen as has been observed before.[22,32,33] The spectral narrowing occurs on ∼30 ps time scale. In separate experiments using ns-laser excitation with a cw-IR laser probe, we found that the electrons recombine on the tens of μs time scale (Figure S2A).

The Role of TEOA. TEOA is not just an external (outer-sphere) electron donor in DMF solutions. Instead, under illumination in the presence of TEOA, the $[Re^I(bpy)(CO)_3DMF]^+$ catalyst binds CO_2 in the form of a TEOA-CO_2 carbonate ligand ($[Re^I(bpy)(CO)_3$-$OC(O)O$-$(CH_2)_2NR_2]^0$; Scheme 1). Ishitani and co-workers showed the analogous ligand exchange process for the homogeneous $[Re^I(bpy)(CO)_3DMF]^+$ catalyst in the presence of TEOA and CO_2 by using FTIR and ESI-MS measurements.[30] On the basis of their findings and FTIR spectra, we could confirm the formation of TiO_2–$[Re^I(bpy)(CO)_3$-$OC(O)O$-$(CH_2)_2NR_2]^0$ under irradiation in the presence of TEOA and CO_2 (Figure S3A, S3C, and Scheme 1). Fs-TRIR spectroscopy also shows that, after ligand exchange, the new species $[Re^I(bpy)(CO)_3$-$OC(O)O$-$(CH_2)_2NR_2]^0$ is able to inject electrons to TiO_2 (Figure S3B and S3D). The ultrafast electron injection has the same amplitude with and without TEOA and CO_2 indicating that the injecting species is the major species (Figure S3E).

Moreover, we found that for TiO_2–$[Re^I(bpy)(CO)_3$-$OC(O)O$-$(CH_2)_2NR_2]^0$ the oxidized catalyst TRIR peak on the high wavenumber side of the GSB is absent, whereas the electrons are clearly present in the CB of TiO_2. Thus, the TEOA-ligand seems to be able to reduce the oxidized catalyst on the same time scale as the electron injection process, forming the species where the "hole" has moved to the TEOA ligand: $TiO_2(e^-)$–$[Re^I(bpy)(CO)_3$-$OC(O)O$-$(CH_2)_2N^{\bullet+}R_2]^+$. Figure 1C shows the TRIR spectra of TiO_2–$[Re^I(bpy)(CO)_3$-$OC(O)O$-$(CH_2)_2NR_2]^0$ where the e^-_{CB} signal at 2100 cm^{-1} has been subtracted to emphasize the molecular signals. The CO signals of $TiO_2(e^-)$–$[Re^I(bpy)(CO)_3$-$OC(O)O$-$(CH_2)_2N^{\bullet+}R_2]^+$ are upshifted compared to those of the ground state complex, consistent with formation of a cation radical in the vicinity of the Re^I center. We note that the spectra are similar to those of the $(bpy^-)Re^{II}$ MLCT state on ZrO_2, but they are more narrow and do not show the same shift with time as the MLCT state on ZrO_2. For the TiO_2 sample, the peak stabilizes at 2036 ± 1 cm^{-1} within 1 ps, whereas the ZrO_2 sample red-shifts by 10 cm^{-1} during 500 ps (see Figure S4). The signal of $TiO_2(e^-)$–$[Re^I(bpy)(CO)_3$-$OC(O)O$-$(CH_2)_2N^{\bullet+}R_2]^+$ should therefore not be mistaken for an MLCT state.

The reactions were followed on a longer time scale using a ns-laser/TRIR setup. Figure 2 compares the TRIR spectra of TiO_2–$[Re^I(bpy)(CO)_3DMF]^+$ without (2A) and with (2B) TEOA and CO_2. At first sight, in Figure 2A, we can recognize the GSB peak and the oxidized catalyst peak $TiO_2(e^-)$–$[Re^{II}(bpy)(CO)_3DMF]^{2+}$ on the higher wavenumber side, which agrees well with the fs-FTIR results of Figure 1A. These signals decay on a time scale of a few μs. In contrast, after introducing TEOA and CO_2, we found that, in addition to the GSB of $TiO_2(e^-)$–$[Re^I(bpy)(CO)_3$-$OC(O)O$-$(CH_2)_2NR_2]^0$[30] at 2020 cm^{-1}, an absorption peak appears on the lower wavenumber side, and this grows stronger during the first few 100s of ns. This means an increased electron density on the Re center and can be attributed to a singly reduced catalyst.[34,35] Our assignment is based on the following spectral analysis. We subtract the spectrum at 50 ns from the spectrum at 5000 ns for the TiO_2-catalyst samples with and without TEOA/CO_2 (Figure S3F). The resulting peak at 2015 cm^{-1} for the sample with TEOA/CO_2 is in good agreement with the results of Kubiak and co-workers,[34] who reported the FTIR spectrum of the singly reduced species $[(^tbu_2\text{-bpy})(CO)_3ReCl]^-$ ($^tbu_2$-bpy =4,4′-di-*tert*-butyl-2,2′-bipyridine), where the added electron density centered mostly on the bipyridine ligand.[34] The electron density on the Re center induced by the anionic Cl^- ligand in their work is matched by the carbonate ligand in the present case. The doubly oxidized TEOA (R_2-N-$(CH_2)_2OH$) is formed via deprotonation and rearrangement to the corresponding R_2N^+ = CH–$CH_2OC(O)O^-$ species. Thus, we propose the structural notation $TiO_2(e^-)$–$[Re^I(bpy^-)(CO)_3$-$OC(O)O$-$CH_2CHN^+R_2]^0$ for the reduced catalyst species from which one proton has been released. Note that the formation of the singly reduced catalyst is not at the expense of the electrons in the TiO_2 CB as the entire background absorption increases on the same time scale (Figure 2B). The only other plausible electron source for catalyst reduction is the oxidized TEOA

DOI: 10.1021/jacs.6b11308
J. Am. Chem. Soc. 2017, 139, 1226–1232

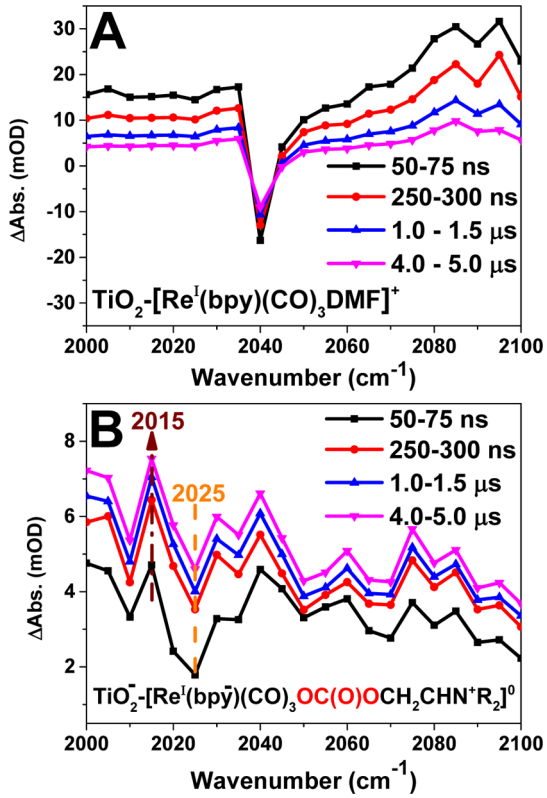

Figure 2. ns-TRIR spectra at different time delays after the photoexcitation for (A) TiO_2–$[Re^I(bpy)(CO)_3DMF]^+$ and (B) TiO_2–$[Re^I(bpy)(CO)_3]$ in the presence of TEOA/CO_2. The molecular GSB is at 2040 and 2025 cm^{-1}, respectively, in agreement with the FTIR spectra. In (B) is also marked the peak at 2015 cm^{-1} for the singly reduced catalyst $TiO_2(e^-)$–$[Re^I(bpy^-)(CO)_3$-$OC(O)O$-$CH_2CHN^+R_2]^0$.

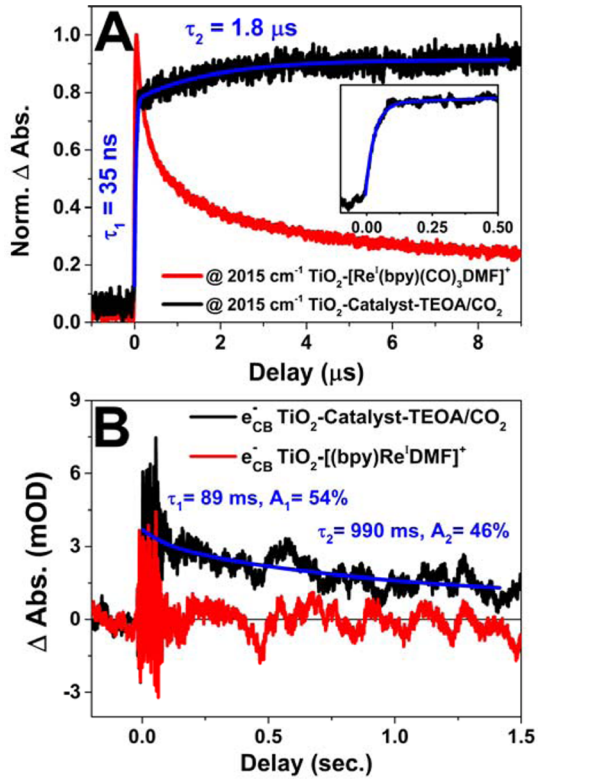

Figure 3. (A) Traces at 2015 cm^{-1} for TiO_2 catalyst (red) and for TiO_2 calayst in the presence of TEOA and CO_2 (black) up to 10 μs (inset: showing the rising component) and (B) traces at 2100 cm^{-1} (electrons in TiO_2 CB) for TiO_2 catalyst (red) and TiO_2 catalyst in the presence of TEOA/CO_2 (black) up to 1.5 s delay after the photoexcitation.

radical $[OC(O)O(CH_2)_2NR_2]^{\bullet+}$ that is unstable and highly reducing, such that each TEOA can donate two equivalents of electrons.[36−39] On ZrO_2 instead, there was no measurable formation of the singly reduced catalyst on this time scale (Figure S3F). This finding confirms that electron injection from $[Re^I(bpy)(CO)_3$-$OC(O)O$-$(CH_2)_2NR_2]^+$ into TiO_2 plays a role in the photoreduction process. This triggers the first oxidation of TEOA on a ps time scale and releases a second equivalent of electrons on a time scale of ∼1 μs. The second equivalent mostly reduces the Re catalyst but some apparently ends up as CB electron. This can possibly be explained by the close proximity of the re-coordinated TEOA to TiO_2 or by prior decoordination of the TEOA radical from the Re complex. Thermodynamically, the TEOA radical has enough reducing power to reduce the Re complex, and consequently, it is able to reduce the CB of TiO_2.[37] Figure 3A compares the traces at 2015 cm^{-1} with and without introducing TEOA/CO_2 corresponding to the transient spectra in Figure 2, which illustrates the differences in reactions on this time scale.

In the absence of TEOA/CO_2, most of the signal from CB electrons in TiO_2 decays within 10 μs by charge recombination with the oxidized catalyst: $TiO_2(e^-)$–$[Re^{II}(bpy)(CO)_3DMF]^{2+}$ → TiO_2–$[Re^I(bpy)(CO)_3DMF]^+$. In the sample with TEOA/CO_2 instead, the electrons in the TiO_2 CB do not show any decay up to tens of ms (Figure 3A and B). From the transient spectra and traces, it is clear that the reduced catalyst $[Re^I(bpy^-)(CO)_3$-$OC(O)O$-$CH_2CHN^+R_2]^0$ forms on a rapid time scale τ_1 = 35 ns followed by a slow rise in Figure 3A (τ_2 = 1.8 μs). At the same time the background signal of CB electrons increases for which the IR extinction coefficient is larger than for the catalyst species (see the relative ΔAbs of the molecular peak vs broad background in Figure 2B).

TiO_2 Role in CO_2 Photoreduction by $[Re^I(bpy)(CO)_3]^+$ Catalyst. The data indicate that there is an electron injection from the excited $[Re^I(bpy)(CO)_3L]^*$ to the TiO_2 CB on a ps time scale. For the sample with TEOA/CO_2, this leads to phototriggered oxidation of TEOA and formation of a reduced catalyst, which is not seen on ZrO_2. Therefore, TiO_2 has an active role in the light-induced electron transfer reactions of this system. To further investigate the role of TiO_2, we probed the destiny of CB electrons on longer time scales.

Figure 3B compares the traces at 2100 cm^{-1} (CB electron absorption region) up to 1.5 s after photoexcitation of the TiO_2 catalyst without (red trace) and with introducing TEOA/CO_2 (black trace). Without TEOA/CO_2, no electrons were left in the TiO_2 CB on this time scale, but introduction of TEOA and CO_2 to the attached catalyst changed the kinetics drastically. Clearly, the electrons were still in the TiO_2 CB on this time scale, and only around 50% of the electrons had disappeared from the CB after around 100 ms, whereas the remaining 50% decayed with $\tau \approx 1$ s. This time scale ($\tau \approx 1$ s) is very similar to that reported for decay of the reduced catalyst signal (τ = 0.4 s) at 500 nm (bpy^-Re^I signal)[21] even though we could not follow the molecular signal by mid-IR on the ms to seconds time scale. It is important to note that there is no accumulation of more reduced catalyst species upon repeated laser flashing or continuous irradiation. Thus, we propose that the CB electrons

DOI: 10.1021/jacs.6b11308
J. Am. Chem. Soc. 2017, 139, 1226−1232

are added to the reduced catalyst and lead to catalytic turnover, restoring the sample to the initial TiO_2–[$Re^I(bpy)(CO)_3$-$OC(O)O$-$(CH_2)_2NR_2]^0$ state; we discuss a possible mechanism in the next section. At present, we do not know if the CB electrons that decay with $\tau \approx 89$ ms also contribute to catalyst reduction or if they are lost in side reactions. In any case, these experiments add more evidence that TiO_2 plays a role in the photocatalytic reduction of CO_2 in this system other than being a scaffold. In this context, we note again that formation of the singly reduced catalyst $[Re^I(bpy^-)(CO)_3$-$OC(O)O$-$(CH_2)_2N^{\bullet+}R_2]^0$ on ZrO_2, by quenching of the excited Re complex by the appended TEOA was not measurable (Figure S3F), which means that the electron injection process in TiO_2 promotes formation of this species. This agrees well with the differences in catalytic activity of the catalyst on TiO_2 and on ZrO_2.[21]

Proposed Photocatalytic Mechanism. The mechanism of CO_2 reduction by $[Re^I(bpy)(CO)_3L]$ catalysts is still under debate with different mechanistic pathways being discussed.[8,35,40,41] Under electrocatalytic reduction conditions, the complex typically undergoes a two-electron reduction and loses the labile ligand (L) to form a $[Re(bpy)(CO)_3]^-$ species that binds to CO_2 and enters the catalytic cycle.[41] However, under photocatalytic reduction conditions, the one-electron-reduced complex $[Re^0(bpy)(CO)_3]$ may already bind to CO_2 and start the catalytic cycle.[42] Attaching the catalyst to TiO_2 improves the catalytic activity but also further increases the mechanistic complexity. Scheme 2 presents our proposed mechanism of the photocatalytic reduction of CO_2 using the TiO_2–$[Re^I(bpy)(CO)_3DMF]^+$ system in the presence of TEOA/CO_2 in DMF solution. As shown above, TiO_2–$[Re^I(bpy)(CO)_3]^+$ is able to capture CO_2 and bind it as a carbonated TEOA ligand, forming the catalyst TiO_2–$[Re^I(bpy)(CO)_3$-$OC(O)O$-$(CH_2)_2NR_2]^0$. Upon photoexcitation of this complex, electron injection into the CB of TiO_2 occurs on the ps time scale. This is rapidly followed by electron transfer from the bound TEOA ligand $[-(CH_2)_2NR_2]$ to the oxidized catalyst to form $TiO_2(e^-)$–$[Re^I(bpy)(CO)_3$-$OC(O)O$-$(CH_2)_2N^+R_2]^+$. On a ns-μs time scale, the $(-(CH_2)_2NR_2)^{\bullet+}$ radical cation shifts the radical from the nitrogen to an adjacent carbon that deprotonates and donates a second electron to further reduce the complex and form $TiO_2(e^-)$–$[Re^I(bpy^-)$-$(CO)_3$-$OC(O)O$-$CH_2CHN^+R_2]^0 + H^+$. This must be followed by release of the oxidized TEOA to form the CO_2-bound catalyst $TiO_2(e^-)$–$[Re^{II}(bpy)(CO)_3CO_2]^0$, where the CO_2 carbon now coordinates to the Re center and two reducing equivalents are located on the CO_2 group. The CO_2 may be derived from the carbonate-TEOA ligand that loses TEOA and rearranges to carbon coordination. Alternatively, the entire ligand decoordinates to form the one-electron-reduced, 17-electron species $TiO_2(e^-)$–$[Re^I(bpy^-)(CO)_3]^0$ that then binds another CO_2 molecule. Both pathways end up forming the critical $TiO_2(e^-)$–$[Re^{II}(bpy)(CO)_3CO_2]^0$ species. On a time scale of ms to seconds, electrons in the CB of TiO_2 reduce $[Re^{II}(bpy)(CO)_3CO_2]^0$ to form the metallocarboxylate intermediate species TiO_2–$[Re^I(bpy)(CO)_3CO_2]^-$. The metallocarboxylate intermediate can undergo a protonation (from TEOA/DMF) followed by loss of H_2O to generate TiO_2–$[Re^I(bpy)(CO)_3CO]^+$.[42] This 18-electron species must be reduced before CO is released and the starting complex is regenerated. The question is where does this final electron come from under our experimental conditions. On the basis of results from Kubiak and co-workers,[35] we suggest that a small fraction of electron equivalents from the TiO_2 CB could catalytically reduce the entire population of $[Re^I(bpy)$-$(CO)_3CO]^+$.

Scheme 2. Proposed Photocatalytic Mechanism of the $[Re^I(bpy)(CO)_3]^+$ Catalyst Attached to the TiO_2 Surface for CO_2 Reduction[a]

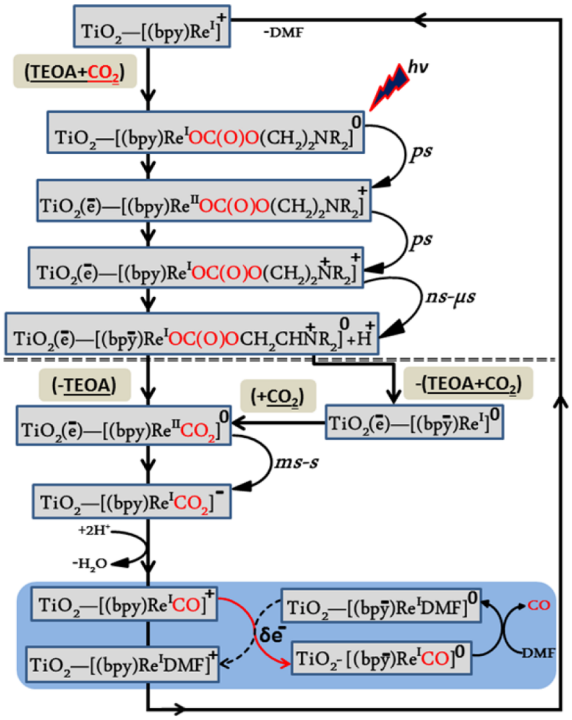

[a]The states formed on the ps-μs time scale were spectroscopically observed (above the dashed line), whereas the remaining species (below the dashed line) are suggested based on published mechanisms to complete catalytic turnover (see text). For simplicity of notation, we ignore the $(CO)_3$ groups in the catalyst chemical structure in this scheme.

Kubiak and co-workers found that substoichiometric amounts (~0.1 equiv) of reductant were sufficient to convert an entire sample of $[Re^I(bpy)(CO)_3CO]^+$ to $[Re^I(bpy)$-$(CO)_3DMF]^+$ in homogeneous solution. They presented a mechanism with an electron-transfer-catalyzed ligand exchange.[35] Formation of TiO_2–$[Re^I(bpy^-)(CO)_3CO]^0$ in a small amount leads to replacement of CO with solvent molecule (DMF) to form TiO_2–$[Re^I(bpy^-)(CO)_3DMF]^0$. This complex is more reducing than the CO complex and therefore undergoes electron transfer with TiO_2–$[Re^I(bpy)$-$(CO)_3CO]^+$ to propagate the reduction-ligand exchange process according to the small loop presented in Scheme 2.[35] Finally, TiO_2–$[Re^I(bpy)(CO)_3DMF]^+$ binds TEOA and CO_2 to reform the starting material as it was before laser flash initiation. Note that the scheme does not indicate all possible charge recombination steps and other loss pathways, which presumably make the overall quantum yield much less than 100%. The most interesting part of the proposed mechanism is that the catalyst is able to inject electrons to TiO_2, and when the catalyst becomes reduced by TEOA, it can accept the electron back. This explains the redox active role of TiO_2 as an electron reservoir in the TiO_2 catalyst system in the presence of TEOA and CO_2.

DOI: 10.1021/jacs.6b11308
J. Am. Chem. Soc. 2017, 139, 1226–1232

CONCLUSIONS

We have shown that TiO_2 plays an important and active role in the photocatalytic reduction of CO_2 by the $[Re^I(bpy)(CO)_3L]^+$ catalyst in DMF and TEOA. First, the electron injection from the excited catalyst to TiO_2 is followed by rapid and efficient regeneration of the Re^I center by the attached TEOA ligand. A second electron transfer, from the TEOA radical cation, leads to formation of the singly reduced $[Re^I(bpy^-)(CO)_3L]$ species on a time scale of 35 ns. We propose that the increase in photocatalytic activity observed when the catalyst is bound to TiO_2, as compared to ZrO_2 or in homogeneous solution,[21] is due to the slow charge recombination and high oxidative power of the Re^{II} species after injection as compared to the excited MLCT state on ZrO_2 or in solution, which results in a more efficient reaction with TEOA. Second, it seems that TiO_2 works as an electron bank that is able to accept, save, and give back the electrons to the catalyst and thus to help complete the photochemical reduction of CO_2.

ASSOCIATED CONTENT

Supporting Information

The Supporting Information is available free of charge on the ACS Publications website at DOI: 10.1021/jacs.6b11308.

Steady-state absorption, emission, IR spectroscopy, and complementray time-resolved IR spectroscopic data (PDF)

AUTHOR INFORMATION

Corresponding Authors

*Mohamed.Qenawy@kemi.uu.se

*Leif.Hammarstrom@kemi.uu.se

ORCID

Erwin Reisner: 0000-0002-7781-1616

Leif Hammarström: 0000-0002-9933-9084

Notes

The authors declare no competing financial interest.

ACKNOWLEDGMENTS

The authors are grateful for funding from the Knut and Alice Wallenberg Foundation, the Swedish Energy Agency, the Swedish Research Council, the Austrian Christian Doppler Research Association (Austrian Federal Ministry of Science, Research and Economy and the National Foundation for Research, Technology and Development), and the OMV Group. Dr. Mohammad Mirmohades, Jens Föhlinger, and Luca D'Amario are acknowledged for their help with fs-TRIR and ns-FTIR. Prof. Sascha Ott is also acknowledged for his helpful discussion. We are dedicating this work to the soul of Prof. Ahmed Zewail.

REFERENCES

(1) Field, C. B., Barros, V. R., Dokken, D. J., Mach, K. J., Mastrandrea, M. D., Bilir, T. E., Chatterjee, M., Ebi, K. L., Estrada, Y. O., Genova, R. C., Girma, B., Kissel, E. S., Levy, A. N., MacCracken, S., Mastrandrea, P. R., White, L. L., Eds.; *Climate Change 2014: Impacts, Adaptation, and Vulnerability. Part A: Global and Sectoral Aspects. Contribution of Working Group II to the Fifth Assessment Report of the Intergovernmental Panel on Climate Change*; Cambridge University Press: Cambridge, United Kingdom and New York, NY, USA, 2014.

(2) Riplinger, C.; Sampson, M. D.; Ritzmann, A. M.; Kubiak, C. P.; Carter, E. A. *J. Am. Chem. Soc.* **2014**, *136*, 16285.

(3) Roldan, A.; Hollingsworth, N.; Roffey, A.; Islam, H. U.; Goodall, J. B. M.; Catlow, C. R. A.; Darr, J. A.; Bras, W.; Sankar, G.; Holt, K. B.; Hogarth, G.; de Leeuw, N. H. *Chem. Commun.* **2015**, *51*, 7501.

(4) Takeda, H.; Koizumi, H.; Okamoto, K.; Ishitani, O. *Chem. Commun.* **2014**, *50*, 1491.

(5) Won, D.-I.; Lee, J.-S.; Ji, J.-M.; Jung, W.-J.; Son, H.-J.; Pac, C.; Kang, S. O. *J. Am. Chem. Soc.* **2015**, *137*, 13679.

(6) Appel, A. M.; Bercaw, J. E.; Bocarsly, A. B.; Dobbek, H.; DuBois, D. L.; Dupuis, M.; Ferry, J. G.; Fujita, E.; Hille, R.; Kenis, P. J. A.; Kerfeld, C. A.; Morris, R. H.; Peden, C. H. F.; Portis, A. R.; Ragsdale, S. W.; Rauchfuss, T. B.; Reek, J. N. H.; Seefeldt, L. C.; Thauer, R. K.; Waldrop, G. L. *Chem. Rev.* **2013**, *113*, 6621.

(7) Sahara, G.; Ishitani, O. *Inorg. Chem.* **2015**, *54*, 5096.

(8) Morris, A. J.; Meyer, G. J.; Fujita, E. *Acc. Chem. Res.* **2009**, *42*, 1983.

(9) Windle, C. D.; Campian, M. V.; Duhme-Klair, A.-K.; Gibson, E. A.; Perutz, R. N.; Schneider, J. *Chem. Commun.* **2012**, *48*, 8189.

(10) Windle, C. D.; Perutz, R. N. *Coord. Chem. Rev.* **2012**, *256*, 2562.

(11) Figueiredo, M. C.; Ledezma-Yanez, I.; Koper, M. T. M. *ACS Catal.* **2016**, *6*, 2382.

(12) Li, C. W.; Kanan, M. W. *J. Am. Chem. Soc.* **2012**, *134*, 7231.

(13) White, J. L.; Baruch, M. F.; Pander Iii, J. E.; Hu, Y.; Fortmeyer, I. C.; Park, J. E.; Zhang, T.; Liao, K.; Gu, J.; Yan, Y.; Shaw, T. W.; Abelev, E.; Bocarsly, A. B. *Chem. Rev.* **2015**, *115*, 12888.

(14) Woolerton, T. W.; Sheard, S.; Reisner, E.; Pierce, E.; Ragsdale, S. W.; Armstrong, F. A. *J. Am. Chem. Soc.* **2010**, *132*, 2132.

(15) Woolerton, T. W.; Sheard, S.; Pierce, E.; Ragsdale, S. W.; Armstrong, F. A. *Energy Environ. Sci.* **2011**, *4*, 2393.

(16) Manbeck, G. F.; Muckerman, J. T.; Szalda, D. J.; Himeda, Y.; Fujita, E. *J. Phys. Chem. B* **2015**, *119*, 7457.

(17) Agarwal, J.; Fujita, E.; Schaefer, H. F.; Muckerman, J. T. *J. Am. Chem. Soc.* **2012**, *134*, 5180.

(18) Kumar, B.; Llorente, M.; Froehlich, J.; Dang, T.; Sathrum, A.; Kubiak, C. P. *Annu. Rev. Phys. Chem.* **2012**, *63*, 541.

(19) Pastor, E.; Pesci, F. M.; Reynal, A.; Handoko, A. D.; Guo, M.; An, X.; Cowan, A. J.; Klug, D. R.; Durrant, J. R.; Tang, J. *Phys. Chem. Chem. Phys.* **2014**, *16*, 5922.

(20) Hawecker, J.; Lehn, J.-M.; Ziessel, R. *J. Chem. Soc., Chem. Commun.* **1983**, 536.

(21) Windle, C. D.; Pastor, E.; Reynal, A.; Whitwood, A. C.; Vaynzof, Y.; Durrant, J. R.; Perutz, R. N.; Reisner, E. *Chem. - Eur. J.* **2015**, *21*, 3746.

(22) She, C.; Guo, J.; Lian, T. *J. Phys. Chem. B* **2007**, *111*, 6903.

(23) Nahhas, A. E.; Cannizzo, A.; Mourik, F. v.; Blanco-Rodríguez, A. M.; Záliš, S.; Vlček, J. A.; Chergui, M. *J. Phys. Chem. A* **2010**, *114*, 6361.

(24) El Nahhas, A.; Consani, C.; Blanco-Rodríguez, A. M.; Lancaster, K. M.; Braem, O.; Cannizzo, A.; Towrie, M.; Clark, I. P.; Záliš, S.; Chergui, M.; Vlček, A. *Inorg. Chem.* **2011**, *50*, 2932.

(25) Asbury, J. B.; Hao, E.; Wang, Y.; Lian, T. *J. Phys. Chem. B* **2000**, *104*, 11957.

(26) Antila, L. J.; Santomauro, F. G.; Hammarstrom, L.; Fernandes, D. L. A.; Sa, J. *Chem. Commun.* **2015**, *51*, 10914.

(27) Mirmohades, M.; Pullen, S.; Stein, M.; Maji, S.; Ott, S.; Hammarström, L.; Lomoth, R. *J. Am. Chem. Soc.* **2014**, *136*, 17366.

(28) Mirmohades, M.; Adamska-Venkatesh, A.; Sommer, C.; Reijerse, E.; Lomoth, R.; Lubitz, W.; Hammarström, L. *J. Phys. Chem. Lett.* **2016**, *7*, 3290.

(29) Kirgan, R. A.; Sullivan, B. P.; Rillema, D. P. In *Photochemistry and Photophysics of Coordination Compounds II*; Balzani, V., Campagna, S., Eds.; Springer Berlin Heidelberg: Berlin, Heidelberg, 2007; p 45.

(30) Morimoto, T.; Nakajima, T.; Sawa, S.; Nakanishi, R.; Imori, D.; Ishitani, O. *J. Am. Chem. Soc.* **2013**, *135*, 16825.

(31) Wang, Y.; Asbury, J. B.; Lian, T. *J. Phys. Chem. A* **2000**, *104*, 4291.

(32) Anderson, N. A.; Lian, T. *Coord. Chem. Rev.* **2004**, *248*, 1231.

(33) Anderson, N. A.; Ai, X.; Lian, T. *J. Phys. Chem. B* **2003**, *107*, 14414.

(34) Smieja, J. M.; Kubiak, C. P. *Inorg. Chem.* **2010**, *49*, 9283.

DOI: 10.1021/jacs.6b11308
J. Am. Chem. Soc. 2017, 139, 1226−1232

(35) Grice, K. A.; Gu, N. X.; Sampson, M. D.; Kubiak, C. P. *Dalton Trans.* **2013**, *42*, 8498.
(36) Reithmeier, R.; Bruckmeier, C.; Rieger, B. *Catalysts* **2012**, *2*, 544.
(37) Takeda, H.; Koike, K.; Inoue, H.; Ishitani, O. *J. Am. Chem. Soc.* **2008**, *130*, 2023.
(38) Amouyal, E. *Sol. Energy Mater. Sol. Cells* **1995**, *38*, 249.
(39) Lehn, J. M.; Sauvage, J.; Gauthier-Villars: Paris, France, 1977; Vol. *1*, p 449.
(40) Kou, Y.; Nabetani, Y.; Masui, D.; Shimada, T.; Takagi, S.; Tachibana, H.; Inoue, H. *J. Am. Chem. Soc.* **2014**, *136*, 6021.
(41) Sampson, M. D.; Froehlich, J. D.; Smieja, J. M.; Benson, E. E.; Sharp, I. D.; Kubiak, C. P. *Energy Environ. Sci.* **2013**, *6*, 3748.
(42) Schneider, T. W.; Ertem, M. Z.; Muckerman, J. T.; Angeles-Boza, A. M. *ACS Catal.* **2016**, *6*, 5473.

DOI: 10.1021/jacs.6b11308
J. Am. Chem. Soc. 2017, 139, 1226−1232